

# Short-time universal scaling in an isolated quantum system after a quench

Alessio Chiocchetta<sup>a</sup>, Marco Tavora<sup>b</sup>, Andrea Gambassi<sup>a</sup> and Aditi Mitra<sup>b</sup>

<sup>a</sup>*SISSA — International School for Advanced Studies and INFN, via Bonomea 265, 34136 Trieste, Italy and*

<sup>b</sup>*Department of Physics, New York University, 4 Washington Place, New York, NY 10003, USA*

(Dated: January 29, 2022)

Renormalization-group methods provide a viable approach for investigating the emergent collective behavior of classical and quantum statistical systems in both equilibrium and nonequilibrium conditions. Within this approach we investigate here the dynamics of an isolated quantum system represented by a scalar  $\phi^4$  theory after a global quench of the potential close to a critical point. We demonstrate the emergence of a transient short-time scaling regime for deep quenches, which is dynamically destabilized by additional relevant terms. This unusual nonthermal regime is characterized by the emergence of short-time universal exponents in the time dependence of the relevant dynamical correlations, which we calculate at the lowest order in a dimensional expansion.

PACS numbers: 05.70.Ln, 64.60.Ht, 64.70.Tg

## I. INTRODUCTION

The nonequilibrium dynamics of isolated, strongly interacting quantum many-body systems is currently under intensive experimental and theoretical investigation (see, e.g., Refs. [1–3]), primarily motivated by recent advances in the physics of cold atomic gases [4]. A natural question which arises in this context concerns the eventual thermalization of these systems after a sudden change (*quench*) of a control parameter. In fact, even though isolated systems evolve with unitary dynamics [5, 6], their local properties can be described, after some time, by suitable statistical ensembles [7–9]. Interestingly enough, the eventual approach to a thermal state might involve intermediate *pre-thermal* quasi-stationary states, proposed theoretically [10] and experimentally observed [11–13]. These states appear to be related to the integrable part of the post-quench Hamiltonian [14–21], which alone [22] would drive the system towards a state, sometimes well described by the so-called generalized Gibbs ensemble (GGE) [23–31]. Inspired by the analogy with renormalization-group (RG) flows, pre-thermalization has been ascribed to a non-thermal unstable fixed-point [32–34] towards which the evolution of the system is attracted before it crosses over to the eventual, stable, thermal fixed point.

While most of the properties of an isolated system after a quench depend on its microscopic features, some acquire a certain degree of universality if the post-quench Hamiltonian is close to a critical point. Examples include the density of defects [1], dynamics of correlation functions [19, 35], statistics of the work [36–38], rephasing dynamics [39], and dynamical phase transitions [40–47]. Despite this progress, an important open issue is the possible emergence of a *universal* collective behavior at *macroscopic short-times* controlled by the memory of the initial state, i.e., a kind of quantum aging. This is known to occur in the presence of a thermal bath both for classical [48–51] and, more recently, quantum [52, 53] statistical systems after a temperature quench which breaks the time-translational invariance (TTI) characteristic of

equilibrium dynamics. The “temporal boundary” introduced by the quench allows the emergence of such a short-time universal scaling, similarly to the case of spatial boundaries in equilibrium systems [54–56]. Here we investigate the extent to which this dynamical feature carries over to quantum systems on their way to (a possible) thermalization in the absence of a thermal bath.

At the lowest order in a dimensional expansion, we construct the RG equations for an *isolated* quantum system after a quench and we discuss the resulting RG flow, comparing it with the equilibrium one at a certain effective temperature  $T_{\text{eff}}$ . Similarly to the case of dissipative systems alluded to above, we show the appearance of universal algebraic laws associated with a non-thermal fixed point approached shortly after a deep quench, which determines the temporal scaling of the relevant correlation functions, and which is later on destabilized by the dynamics.

## II. THE MODEL

We consider a system with Hamiltonian

$$H(r, u) = \int d^d x \left[ \frac{1}{2} \Pi^2 + \frac{1}{2} (\nabla \phi)^2 + \frac{r}{2} \phi^2 + \frac{u}{4!} \phi^4 \right], \quad (1)$$

where  $u > 0$ ,  $\phi$  is a scalar bosonic field with bare square mass  $r$  and  $\Pi$  its conjugate momentum.  $H$  is the continuum limit of a  $d$ -dimensional lattice of coupled anharmonic oscillators. The system is prepared at  $t < 0$  in the ground state of the non-interacting Hamiltonian  $H_0 \equiv H(\Omega_0^2, 0)$  with  $\Omega_0 > 0$  and at time  $t = 0$  the parameters are suddenly changed, resulting in the post-quench Hamiltonian  $H \equiv H(r, u)$ . (Below we assume that  $\bar{\phi}(t) \equiv \langle \phi \rangle$  vanishes during the dynamics.)  $H$  for  $u = 0$  as well as  $H_0$  can be diagonalized in momentum space in terms of two sets of creation/annihilation operators with dispersion relation  $\omega_k(r) = \sqrt{k^2 + r} \equiv \omega_k$  and  $\omega_k(\Omega_0^2) \equiv \omega_k^0$ , respectively, where  $k$  is the modulus of the momentum. By requiring the continuity of  $\phi$  and  $\Pi$  during the quench  $\Omega_0^2 \rightarrow r$ , these two sets are

related by a Bogoliubov transformation [57]. The corresponding retarded ( $R$ ) and Keldysh ( $C$ ) nonequilibrium Green's functions [58]  $iR(1,2) = \theta(t_1 - t_2)\langle[\phi(1), \phi(2)]\rangle$  and  $iC(1,2) = \langle\{\phi(1), \phi(2)\}\rangle$ , with  $i \equiv (\mathbf{x}_i, t_i)$ , are

$$R(k, t_1, t_2) = -\theta(t_-) \sin(\omega_k t_-) / \omega_k, \quad (2)$$

$$iC(k, t_1, t_2) = [K_+ \cos(\omega_k t_-) + K_- \cos(\omega_k t_+)] / \omega_k, \quad (3)$$

for  $u = 0$  and in Fourier space, where  $t_{\pm} = t_1 \pm t_2$  and  $K_{\pm}(k) = (\omega_k / \omega_k^0 \pm \omega_k^0 / \omega_k) / 2$ . Note that  $C$  (but not  $R$ ) depends on the state before the quench and is not TTI. Hereafter we primarily focus on the case of a deep quench  $\Omega_0 \gg \Lambda$ , where  $\Lambda$  is the momentum cutoff introduced further below. The stationary part  $\Omega_0 \cos(\omega_k t_-) / (2\omega_k^2)$  of  $iC$  turns out to have the same form as the equilibrium  $iC$  [57] at high temperature  $T = \Omega_0 / 4 \gg \Lambda$  (see also Refs. [59, 60]). A similar conclusion holds for the (non-thermal) occupation number  $n_k$  of the post-quench momenta, which is approximately thermal at low momenta. Accordingly, the possible emerging collective behavior of the system after the quench is expected to bear some similarities to the equilibrium transition. The latter occurs at a value  $r_{\text{eq}}^*(T)$  of  $r$  which depends on the temperature  $T$  [61–63] and it displays the critical properties of its universality class in  $d$  spatial dimensions for  $T > 0$ , in contrast to the  $d+1$  dimensions at  $T = 0$ . Thus, after the quench, one expects a collective behavior to emerge at some value  $r^*(\Omega_0)$  of  $r$ , with an upper critical dimensionality  $d_c = 4$ . In addition, the non-stationary part  $-\Omega_0 \cos(\omega_k t_+) / (2\omega_k^2)$  of  $iC$  (absent in equilibrium) turns out to be responsible for the short-time universal scaling behavior investigated below.

### III. RENORMALIZATION-GROUP FLOW

In order to highlight the emergence of dynamical scaling after the quench, we study the RG flow of the relevant couplings within a perturbative approach based on the Schwinger-Keldysh formalism [58]. In particular, from  $H$  in Eq. (1) we construct the action describing the nonequilibrium behavior of the system. Then we determine the effective action for the “slow modes” by integrating out the fast ones characterized by a momentum  $k$  within a shell of infinitesimal thickness below the large-momentum cutoff  $\Lambda$ . Subsequently, spatial coordinates, time, and fields are rescaled in order to restore the initial cutoff  $\Lambda$ : from the resulting coupling constant one infers the RG equations [64, 65]. An analogous procedure was recently carried out after a quench in  $d = 1$  [19, 66]. The one-loop RG equations up to the first order in  $u$  and at intermediate times ( $\Lambda^{-1} \ll t \ll t^*$  with  $t^*$  discussed later) are

$$\frac{dr}{d\ell} = 2r + \frac{a_d}{8} u \Lambda^d \frac{2\Lambda^2 + r + \Omega_0^2}{(\Lambda^2 + r) \sqrt{\Lambda^2 + \Omega_0^2}} + \mathcal{O}(u^2), \quad (4a)$$

$$\frac{du}{d\ell} = (d_c - d)u - \frac{3a_d}{8} u^2 \Lambda^{d-4} \sqrt{\Lambda^2 + \Omega_0^2} + \mathcal{O}(u^3), \quad (4b)$$

where  $a_d = 2 / [(4\pi)^{d/2} \Gamma(d/2)]$  and  $\ell > 0$  is the flow parameter which rescales coordinates and times as  $(x, t) \mapsto (e^{-\ell} x, e^{-\ell} t)$ . These RG equations encompass the cases of shallow ( $\Omega_0 \ll \Lambda$ ) and deep ( $\Omega_0 \gg \Lambda$ ) quenches. In the former, inspection of Eq. (4b) shows that the effective coupling constant is  $u \Lambda^{d-3}$  and therefore the upper critical dimensionality is  $d_c = 3$ , i.e., the same as in equilibrium at  $T = 0$ . In the latter, instead, the effective coupling is  $\Omega_0 u \Lambda^{d-4} \equiv 16g / a_d$  and, correspondingly,  $d_c = 4$ . This kind of *dimensional crossover* is similar to the one occurring in equilibrium quantum systems upon varying  $T$  [61–63] (or in classical statistical systems in spatial confinement, see, e.g., Ref. [67]). However, while for equilibrium systems  $T$  does not flow under RG [63] due to the presence of the thermal bath, in the present case  $\Omega_0$  is renormalized by the interaction because of the non-stationary terms in  $iC$ . In particular, for a deep quench, the flow of  $\Omega_0$  calculated as outlined above is

$$\frac{d\Omega_0}{d\ell} = -\frac{a_d}{16} \Omega_0^2 u \Lambda^{d-4} + \mathcal{O}(u^2) = -g \Omega_0 + \mathcal{O}(g^2). \quad (5)$$

Correspondingly,  $g \propto \Omega_0 u$  flows according to Eqs. (4b) and (5), which yield, together with Eq. (4a),

$$d\rho/d\ell = 2\rho + 2g/(1 + \rho) + \mathcal{O}(g^2), \quad (6a)$$

$$dg/d\ell = \epsilon g - 7g^2 + \mathcal{O}(g^3), \quad (6b)$$

where  $\epsilon \equiv 4 - d$  and  $\rho \equiv r / \Lambda^2$ . Equations (6) and (5) establish a flow in the  $(\rho, g, \Omega_0)$ -space and they admit an  $\Omega_0$ -independent non-Gaussian fixed-point  $P \equiv (\rho^*, g^*) = (-\epsilon/7, \epsilon/7) + \mathcal{O}(\epsilon^2)$  in the  $(\rho, g)$ -plane, which, for  $\epsilon > 0$ , is approached upon increasing  $\ell$  if the flow starts from a point on the stable manifold (critical line) associated with  $P$  (see Appendix A). By linearizing Eqs. (6) around  $P$ , one determines the exponent  $\nu = 1/2 + \epsilon/14 + \mathcal{O}(\epsilon^2)$  controlling the flow along the unstable direction in the  $(g, \rho)$ -plane, which differs from the equilibrium value  $\nu_{\text{eq}} = 1/2 + \epsilon/12 + \mathcal{O}(\epsilon^2)$  at  $T \neq 0$ . Although  $g \simeq g^*$ , the coupling  $u \propto g^* \Omega_0^{-1}(\ell)$  of  $H$  keeps flowing, in contrast to the cases of quenches of classical or quantum systems in contact with thermal baths in which the temporal boundary does not affect the behavior of  $u$  [48, 49, 52].

Note that Eq. (5) implies that  $\Omega_0(\ell)$  simultaneously decreases as  $\Omega_0(\ell) \simeq \Omega_0 e^{-g^* \ell}$ . Due to this downward flow of  $\Omega_0(\ell)$ , the deep-quench regime is eventually left for  $\ell \gtrsim \ell_{\text{dq}} \simeq (1/g^*) \ln(\Omega_0/\Lambda)$ , as sketched in Fig. 1, with  $g$  restarting its flow possibly towards another fixed point. In order to understand heuristically the eventual fate of  $\Omega_0(\ell)$  note that in the opposite case of a shallow quench  $\Omega_0 \ll \Lambda$  a dimensional crossover towards  $d_c = 3$  occurs and therefore for  $d \simeq 4 > d_c$  the scaling is determined by the Gaussian fixed point, which implies  $d\Omega_0/d\ell = \Omega_0$ , i.e.,  $\Omega_0(\ell) \propto e^\ell$  as  $\ell$  increases (lower solid line in Fig. 1). These two competing trends for  $\Omega_0 \gg \Lambda$  and  $\Omega_0 \ll \Lambda$  (which are qualitatively unaffected by the actual value of  $\rho$  and  $g$ ), suggest that  $\Omega_0(\ell)$  might eventually approach a constant at large  $\ell$  (see Fig. 1), as we assume below.

In the regime  $\ell > \ell_{\text{dq}}$ , where  $\Omega_0$  has stopped flowing, Eqs. (4) with  $d_c = 4$  and fixed  $\Omega_0$  are very similar to the

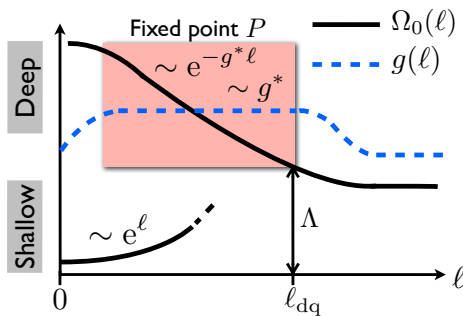


FIG. 1. (Color online) Sketch of the solution of the RG Eqs. (5) and (6) for  $\Omega_0(\ell)$  (solid line) and  $g(\ell)$  (dashed line), along the critical line. After a nonuniversal transient,  $\Omega_0(\ell)$  displays a universal behavior  $\sim e^{-g^* \ell}$  determined by the fixed point  $P$  with  $g(\ell) \simeq g^*$  within the deep-quench regime (red box), which is left for  $\ell \gtrsim \ell_{dq}$ . The lower solid curve indicates the flow of  $\Omega_0(\ell)$  for a shallow quench.

RG equations of the quantum system in equilibrium at  $T \neq 0$  (see, e.g., Ref. [61]) in the classical regime (i.e., for large  $\ell$  such that  $\Lambda e^{-\ell} \leq T$ ) in which  $T$  does not renormalize [63], with  $\Omega_0$  playing the role of a temperature (see Appendix B). In particular, the former and the latter admit the fixed points  $Q(\Omega_0) \equiv (r_{dy}^*(\Omega_0), u_{dy}^*(\Omega_0))$  and  $Q_{eq}(T) \equiv (r_{eq}^*(T), u_{eq}^*(T))$ , respectively, of  $(r, u)$  which describe *dynamical* and *equilibrium* scaling behaviors emerging when  $r$  in Eq. (1) approaches  $r_{dy,eq}^*$ . Remarkably, up to this order in perturbation theory, the critical exponents  $\nu$  derived from these RG equations are the same and they equal  $\nu_{eq}$ . In addition, as discussed in Appendix B, one can define a sort of *effective temperature*  $T = T_{eff}(\Omega_0)$  such that the systems which are critical under equilibrium conditions are also critical after the quench. This implies that the (linearized) critical lines of  $Q$  and  $Q_{eq}$  in the  $(r, u)$ -plane are the same, though  $Q(\Omega_0) \neq Q_{eq}(T_{eff}(\Omega_0))$ . Only for  $\Omega_0 \gg \Lambda$ , these two fixed-points coincide, with  $T_{eff} = \Omega_0/4$  and  $r_{dy}^*(\Omega_0) = r_{eq}^*(T_{eff}) = -\epsilon \Lambda^2/6$ . (In passing, we mention that  $Q(\Omega_0) = Q_{eq}(T_{eff}(\Omega_0))$  also for  $\Omega_0 \ll \Lambda$ , see Appendix B.) In this respect and up to this order in perturbation theory, the dynamical transition (in the notion of Refs. [40–42]) has some of the features of the equilibrium transition occurring at  $T_{eff}$ , though differences could emerge at higher orders in perturbation theory or in quantities which depend on  $Q$  or on the post-quench distribution at short length scales, which is definitely not thermal [45] (see further below). It also remains to be seen whether  $T_{eff}$  has any thermodynamic or dynamic role in the system, e.g., entering into fluctuation-dissipation relations [68, 69].

The RG flow discussed above can be readily translated into a temporal evolution, by taking into account that while the flow parameterized by  $\ell$  progresses, the temporal dependence of the quantities of interest (e.g.,  $C$

and  $R$ ) is rescaled as  $t \mapsto e^{-\ell} t$  and therefore  $\ell \propto \ln(\Lambda t)$  sets the temporal scale. As a consequence, for instance,  $\Omega_0$  acquires an algebraic dependence on time within the deep-quench regime, i.e.,  $\Omega_0(t) \sim t^{-g^*}$ , which eventually affects the behavior of  $C$ ; correspondingly, the deep-quench regime is left for  $\Lambda t \gtrsim \Lambda t_{dq} = (1/g^*) \ln(\Omega_0/\Lambda)$ .

The RG Eqs. (4) and (5) have been derived under the assumption that inelastic scattering does not occur, at least in the early stages of the evolution, and that the dynamical exponent keeps its initial value  $z = 1$ . In fact, up to this order in perturbation theory, the tadpole is the only relevant diagram which is responsible for the occurrence of elastic dephasing during the time evolution and, for a deep quench, it results in the scaling behavior discussed above. However, the RG transformations also generate relevant dissipative terms which are expected to drive the system to thermal equilibrium [70, 71]. In the present case, they appear as secular terms growing in time, eventually spoiling the perturbative expansion (unless they are properly resummed [32, 72, 73]), and changing the dynamical exponent  $z$  towards the diffusive value  $z \simeq 2$ . Nonetheless, these terms — which are absent immediately after the quench and are therefore generated perturbatively — turn out to be small (up to this order in perturbation theory) at short times  $\Lambda t \lesssim \Lambda t^* = 1/g^* \simeq \epsilon^{-1}$ , which include the range of times within which the short-time scaling behavior associated with  $P$  sets in. Note that dissipative terms are not actually generated in the cases studied in Refs. [43–45], whose relevant fluctuations are Gaussian; correspondingly, the scenario sketched in Fig. 1 should apply at all times.

#### IV. SHORT-TIME SCALING OF VARIOUS QUANTITIES

The emergence of a short-time scaling after a deep quench is also revealed by a perturbative calculation of  $iC$  and  $R$  for  $k = 0$ ,  $g = g^*$ , and  $r = r^* \equiv \rho^* \Lambda^2 = -\epsilon \Lambda^2/7 + \mathcal{O}(\epsilon^2)$  (note that  $r^*$  slightly differs from  $r_{dy}^*(\Omega_0 \gg \Lambda)$  discussed above, see also Appendix A). In fact, within the deep-quench regime, it turns out that for  $t_2 \ll t_1$  and up to  $\mathcal{O}(g^{*2})$ ,  $R(0, t_1 \gg t_2) = -t_1[1 - (g^*/2) \ln(t_1/t_2)] \simeq -t_1(t_2/t_1)^\theta$ , where we define  $\theta \equiv g^*/2 = \epsilon/14 + \mathcal{O}(\epsilon^2)$ . Analogously,  $iC(0, t_1, t_2) = \Omega_0 t_1 t_2 [1 - (g^*/2) \ln(\Lambda^2 t_1 t_2)] \simeq (\Omega_0/\Lambda^2)(\Lambda t_2)^{2-2\theta}(t_2/t_1)^{\theta-1}$ . This algebraic dependence on time is analogous to the one observed in classical [49] and quantum [52] systems undergoing *aging* in contact with a thermal bath, with an *initial-slip* exponent  $\theta$ . As in classical systems,  $\theta$  can be related to the anomalous dimension of the fields at the temporal boundary introduced by the quench [74].

The algebraic behavior discussed above affects also other relevant quantities. Consider, for instance, the response function  $R$  as a function of the spatial distance  $x = |\mathbf{x}_1 - \mathbf{x}_2|$ . For  $u = 0$ , its expression  $R^{(0)}(x, t_1 - t_2)$  is TTI and it shows typical light-cone

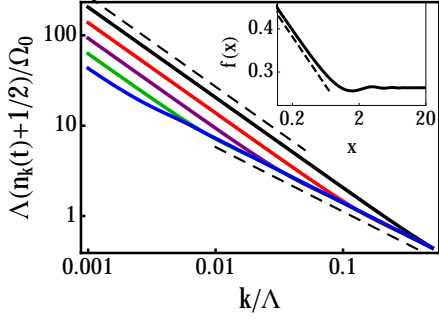


FIG. 2. (Color online) Momentum distribution  $n_k$  after the quench, as a function of  $k/\Lambda \ll 1$  for  $\Lambda t = 2, 8, 32, 128, 512$  (solid lines, from top to bottom). The algebraic short- and long-time behaviors of  $n_k$  are highlighted by the upper  $\sim k^{-1}$  and lower  $\sim k^{-1+2\theta}$  dashed lines, respectively. The inset shows a log-log plot of the scaling function  $f(x)$ , which approaches  $\sim x^{-2\theta}$  for  $x \lesssim 1$  (dashed line). With the purpose of highlighting the crossover, we set  $\epsilon = 2$  in the perturbative expressions of these curves.

dynamics by being enhanced at  $x = t_1 - t_2$  where  $R^{(0)} \propto -\Lambda^3 [\Lambda(t_1 - t_2)]^{-3/2}$  in  $d = 4$ , while decaying rapidly inside the light-cone for  $x \ll t_1 - t_2$ , and being vanishingly small outside it for  $x \gg t_1 - t_2$ . At one loop,  $R$  acquires an algebraic behavior for  $t_2 \ll t_1$ , i.e.,  $R(x = t_1 - t_2, t_2 \ll t_1) \simeq R^{(0)} [1 - \theta \ln(t_1/t_2)] \simeq (t_2/t_1)^\theta t_1^{-3/2}$ .

Analogously, the dynamics of the order parameter  $\bar{\phi}(t) \equiv \langle \phi \rangle$  can be studied by adding a small symmetry breaking field in the pre-quench Hamiltonian  $H(\Omega_0^2, 0) \rightarrow H(\Omega_0^2, 0) - h \int d^d x \phi(x)$ , such that  $\bar{\phi}(0^-) \equiv \phi_0 = h/\Omega_0^2 \ll 1$ . The time evolution of  $\bar{\phi}$  due to the post-quench Hamiltonian  $H$  in Eq. (1) (with no symmetry-breaking field) is determined by  $[\partial_t^2 + M^2(t) - u\bar{\phi}^2/3] \bar{\phi}(t) = 0$  where  $M^2(t) = r + u\bar{\phi}^2/2 + uiC(x=0, t, t)/4$ . At times such that  $\Lambda^{-1} \ll t \ll t_i$  where  $\Lambda t_i \sim \mathcal{O}(1/\sqrt{\bar{\phi}_0^2})$  one finds  $M^2(t) \simeq \theta/t^2$  and therefore  $\bar{\phi} \sim \phi_0 t^\theta$  [74], i.e., the short-time evolution of  $\bar{\phi}$  is controlled by  $\theta$  and corresponds to an initial *increase* of the order with time.

The momentum distribution  $n_k$  of the quasi-particles also shows signatures of the exponent  $\theta$ . Immediately after the quench,  $n_k$  takes the expected form of a GGE with a momentum-dependent effective temperature  $T_{\text{eff}}^k$  [59, 75] which becomes independent of  $k$  and equal to  $T_{\text{eff}}(\Omega_0)$  for deep quenches. Interactions eventually modify this behavior. In particular, within the deep-quench regime with  $g = g^*$  and at the critical point  $r = r^*$ , a perturbative calculation yields  $n_k(t) + 1/2 = (\Omega_0/\Lambda)(\Lambda/k)^{1-2\theta} f(kt)$ , where the scaling function  $f$  can be consistently estimated up to  $\mathcal{O}(\epsilon)$  as the exponential of the one-loop correction and is such that  $f(x \ll 1) \simeq x^{-2\theta}$ , with a finite value for  $x \gg 1$ . Accordingly, at a certain time  $t$ ,  $n_k(t) + 1/2$  as a function of  $k$  crosses over from an algebraic behavior  $\sim k^{-1}t^{-2\theta}$  for  $k \lesssim t^{-1}$  to  $\sim k^{-1+2\theta}$  for  $k \gtrsim t^{-1}$ . This crossover is shown in Fig. 2 along with a plot of  $f(x)$ . It is interesting to note that

the dynamics of  $n_k(t)$  in Fig. 2 closely resemble the one observed at non-thermal fixed points (see, e.g., Ref. [76]).

## V. $O(n)$ AND SPHERICAL MODELS

This perturbative RG analysis can be extended to a Hamiltonian (1) involving  $n$ -component fields  $\vec{\phi}$  and  $\vec{\Pi}$  with an  $O(n)$ -symmetric interaction  $u(\vec{\phi} \cdot \vec{\phi})^2/(4!n)$ . This generalization allows us to take the  $n \rightarrow +\infty$  limit and compare our perturbative results up to  $\mathcal{O}(\epsilon^2)$  with the exact solution of the spherical model. While several studies on this model recently appeared [43–45], its *short-time* universal properties have yet to be explored. Here we fill this gap by highlighting how the results discussed above for  $n = 1$  generalize to  $n \gg 1$ . A more detailed discussion will be presented elsewhere [74]. In the deep-quench regime, the corresponding RG equations for  $\Omega_0$  and  $\rho$  are given by Eqs. (5) and (6a) with  $g \rightarrow g/3$ , while the one for  $g$  is given by Eq. (6b) with  $g \rightarrow g/7$ . As before, a short-time fixed point  $P_\infty = (\rho^*, g^*) = (-\epsilon/3, \epsilon) + \mathcal{O}(\epsilon^2)$  emerges for  $\Omega_0 \gg \Lambda$  and, correspondingly,  $R$  and  $iC$  acquire logarithmic corrections at one-loop which can be resummed via RG. As a result,  $R(k=0, t_1 \gg t_2)$  and  $iC(k=0, t_1, t_2)$  display the same scaling behavior as in the case  $n = 1$  discussed above but with  $\theta$  replaced by  $\theta_\infty = g^*/6 = \epsilon/6 + \mathcal{O}(\epsilon^2)$ . Analogously, in the presence of a tiny initial value  $\bar{\phi}(0^-)$ , the order parameter  $\bar{\phi}$  grows algebraically in time with exponent  $\theta_\infty$ .

## VI. CONCLUSIONS

The RG analysis presented here demonstrates in a simple setting the emergence of a novel scaling behavior after a deep quench of an isolated quantum system. This phenomenon, due entirely to elastic dephasing, is an example of a macroscopic short-time non-thermal fixed point; the corresponding behavior of various physical observables is controlled by a universal exponent  $\theta$ , which we calculated at the first order in a dimensional expansion. The non-thermal fixed point is eventually destabilized by the dynamics itself, which crosses over towards a different thermal-like regime before eventual thermalization occurs, the latter being driven by dissipative terms generated in the effective action.

As the scaling regime unveiled here occurs at short times, its numerical investigation should not be hampered by the computational limitations which typically prevent the investigation of the post-quench dynamics at long times. In addition, our predictions can be tested, e.g., in experimental realizations of the Bose-Hubbard model, belonging to the  $O(2)$  universality class. This model can be actually simulated via ultra-cold atoms in optical lattices [5, 77, 78] or strongly correlated photons/polaritons in arrays of optical cavities [79]. Remarkably, in recent experiments, systems with  $SU(n)$  symmetry have been successfully realized [80, 81]. These may

also serve as possible testing ground to probe the emergence of a short-time universal collective behavior.

### ACKNOWLEDGMENTS

The authors thank I. Carusotto, M. Marcuzzi, and A. Silva for invaluable discussions. MT and AM were supported by NSF-DMR 1303177.

*Note.*— A. C. and M. T. contributed equally to this work.

### Appendix A: Renormalization-group flow

In order to investigate the renormalization-group (RG) flow in more detail it is convenient to introduce the dimensionless variable  $\omega_0 \equiv \Omega_0/\Lambda$  in addition to the dimensionless coupling constant  $g = a_d \Omega_0 u \Lambda^{d-4}/16$  and  $\rho = r/\Lambda^2$  we introduced in the main text. As long as  $\omega_0 \gtrsim 1$ , the upper critical dimensionality of the system is  $d_c = 4$ . The flow equation for  $g$  differs from the one for  $u$  reported in Eq. (4), depending on whether  $\Omega_0$  flows under RG or not. In particular, in the deep quench regime  $\omega_0 \gg 1$ ,  $\omega_0$  does indeed flow according to Eq. (5) with

$$\omega_0(\ell) = \omega_0(0)e^{-\int_0^\ell d\ell' g(\ell')} + \mathcal{O}(g^2), \quad (\text{A1})$$

and the flow equations for  $g$  and  $\rho$  are provided by Eqs. (6), which are actually independent of  $\omega_0$  at least as long as  $\omega_0(\ell) \gg 1$ . These equations admit the non-Gaussian fixed point  $P = (\rho^*, g^*) = (-\epsilon/7, \epsilon/7) + \mathcal{O}(\epsilon^2)$  in the  $(\rho, g)$ -plane, which is indicated by the black vertical line in the  $(\rho, g, \omega_0)$ -space represented in Fig. 3(a). By linearizing Eqs. (6) around  $P$ , one finds that the projected flow on the  $(\rho, g)$ -plane is characterized by a stable direction  $\mathbf{s}_P = (1 - 3\epsilon/28, -1 - 3\epsilon/28)/\sqrt{2} + \mathcal{O}(\epsilon^2)$  and by an unstable one  $\mathbf{u}_P = (1, 0)$ , with eigenvalues  $-\epsilon + \mathcal{O}(\epsilon^2)$  and  $1/\nu$ , respectively. These directions are indicated in Fig. 3(a) by the pairs of arrows pointing, respectively, towards (blue) and away from (red) the vertical line associated with  $P$ . These arrows lie on the corresponding stable and unstable manifold of  $P$ , which are indicated in the figure by the two vertical planes in the  $(\rho, g, \omega_0)$ -space. As expected, if the RG flow originates for  $\ell = 0$  from a point  $O$  which is very close to the stable manifold, the corresponding evolved point  $(\rho(\ell), g(\ell), \omega_0(\ell))$  proceeds downwards and it approaches, as  $\ell$  increases, the stable line which projects onto  $P$ , such that the evolution occurs with  $g(\ell) \simeq g^*$ . However, for larger values of  $\ell$ , the initial (small) distance from the stable manifold is amplified and the trajectory leaves the vertical line along the unstable manifold, as indicated by the solid (green) line in Fig. 3(a). A sketch of the projection of this trajectory onto the  $(g, \omega_0)$ -plane is provided in Fig. 1. Within the range of values of  $\ell$  for which  $g(\ell) \simeq g^*$ , a scaling behavior emerges in the relevant physical quantities and in particular in  $\omega_0(\ell) \propto e^{-g^* \ell}$  (see Eq. (A1)). As we discussed in the main text, upon increasing  $\ell$ ,  $\omega_0(\ell)$  decreases and therefore the deep quench regime is left for

$\ell \gtrsim \ell_{dq}$ , where  $\omega_0(\ell = \ell_{dq}) \simeq 1$ . For  $\ell \gg \ell_{dq}$ , one can expect  $\omega_0(\ell)$  to approach a finite asymptotic value, as a consequence of the competing trends observed for the deep ( $\omega_0 \gg 1$ ) and shallow ( $\omega_0 \ll 1$ ) quenches.

In the stationary regime  $\ell \gg \ell_{dq}$ , Eqs. (4) can be simply rewritten in terms of  $g$ ,  $\rho$ , and the constant  $\omega_0 > 0$

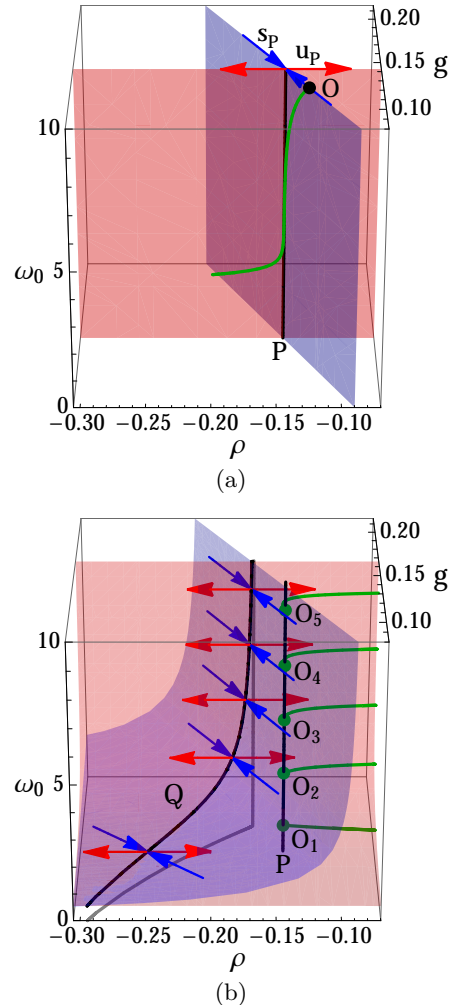


FIG. 3. (Color online) Structure of the RG flow in the  $(\rho, g, \omega_0)$ -space for (a) a deep quench ( $\omega_0 \gg 1$ , with flowing  $\omega_0$ ) and (b) constant  $\omega_0$ . In panel (a), the location on the  $(\rho, g)$ -plane of the fixed point  $P$  is independent of  $\omega_0$  and the corresponding stable (blue) and unstable (red) manifolds are vertical planes. The RG trajectory originating from a point  $O$  close to the stable manifold is indicated by the green line. In panel (b) the RG flow occurs with constant  $\omega_0$  and, upon varying  $\omega_0$ , one identifies a line of fixed points  $Q$  (black solid curve), with the associated stable (blue) and unstable (red) manifolds. The vertical black line corresponds to the fixed point  $P$  of panel (a), while the RG trajectories of a sample of initial points  $O_1, \dots, O_5$  at various values of  $\omega_0$  on that line are indicated in green. See the main text for additional explanations. The curves and surfaces presented in these two panels have been obtained by setting  $\epsilon = 1$  in the perturbative RG Eqs. (6) and (5) (panel (a)) or (B1) (panel (b)).



as

$$\frac{d\rho}{d\ell} = 2\rho + 2g \frac{2 + \rho + \omega_0^2}{\omega_0(1 + \rho)\sqrt{1 + \omega_0^2}} + \mathcal{O}(g^2), \quad (\text{A2a})$$

$$\frac{dg}{d\ell} = \epsilon g - 6g^2 \sqrt{1 + \omega_0^{-2}} + \mathcal{O}(g^3). \quad (\text{A2b})$$

These equations determine a flow in the  $(\rho, g, \omega_0)$ -space which actually occurs at constant  $\omega_0$ , i.e., separately on the various  $(\rho, g)$ -planes. On each of these planes there is a non-Gaussian fixed point  $Q(\omega_0) = (\rho_{\text{dy}}^*(\omega_0), g_{\text{dy}}^*(\omega_0))$  (which is stable for  $\epsilon > 0$ ) with  $\rho_{\text{dy}}^*(\omega_0) = -(\epsilon/6)(2 + \omega_0^2)/(1 + \omega_0^2) + \mathcal{O}(\epsilon^2)$  and  $g_{\text{dy}}^*(\omega_0) = (\epsilon/6)\omega_0/\sqrt{1 + \omega_0^2} + \mathcal{O}(\epsilon^2)$ . This family of fixed points in the  $(\rho, g, \omega_0)$ -space is indicated by the black curve in Fig. 3(b), whose projection on the  $(\rho, g)$ -plane is indicated by the gray curve, together with its vertical asymptote for  $\omega_0 \gg 1$ . Note, however, that larger values of  $\omega_0$  correspond to the deep-quench regime previously discussed, which is controlled by a different set of flow equations and which makes  $\omega_0$  flow towards smaller values. By linearizing Eqs. (A2) around  $Q(\omega_0)$ , one finds that the flow occurring at constant  $\omega_0$  is characterized on the  $(\rho, g)$ -plane by a stable direction  $\mathbf{s}_Q(\omega_0) \propto (\hat{g}(\omega_0), -(1 - \epsilon/3)) + \mathcal{O}(\epsilon^2)$  — with  $\hat{g}(\omega_0) = (2 + \omega_0^2)/[\omega_0\sqrt{1 + \omega_0^2}]$  — and by an unstable one  $\mathbf{u}_Q(\omega_0) = (1, 0)$ , with eigenvalues  $-\epsilon + \mathcal{O}(\epsilon^2)$  and  $2(1 - \epsilon/6) + \mathcal{O}(\epsilon^2) = 1/\nu_{\text{eq}}$ , respectively. These directions are indicated in Fig. 3(b) by various pairs of arrows pointing, respectively, towards (blue) and away from (red) the curve associated with  $Q$ . These arrows lie on the corresponding stable and unstable manifold of  $Q$ , indicated in the figure by the red and blue surfaces, respectively. The vertical black line in Fig. 3(b) corresponds to the same deep-quench fixed-point  $P$  as in panel (a), extrapolated to values of  $\omega_0$  which are not necessarily within the deep-quench regime. Under the effect of the flow in Eq. (A2) it turns out that the points (e.g.,  $O_1, \dots, O_5$ ) along that line — which in principle might be reached by following the flow characterizing the deep-quench regime — will eventually flow towards the large- $\rho$  fixed point, while keeping their original value of  $\omega_0$ . This behavior is highlighted by the five green curves in panel (b), which originate on the line corresponding to  $P$  for various values of  $\omega_0$  at  $O_1, \dots, O_5$ , and which eventually approach the unstable manifold associated with  $Q$  as the RG flow proceeds. Although it seems that starting from a point on the stable manifold of the deep-quench regime (see Fig. 3(a)) its flow is inevitably driven towards the large- $\rho$  fixed point once the flow of  $\omega_0$  stops (see Fig. 3(b)), this might not actually be the case. In fact, as depicted in Fig. 3(a), a trajectory which starts close to that manifold might first display the scaling behavior of  $P$  and then be driven towards the small- $\rho$  phase along the corresponding unstable manifold, which actually intersect the stable one of the family of fixed points with constant  $\omega_0$ . As a result, depending on how the flow of  $\omega_0$  actually stops, it should be possible to find suitable initial conditions

in the deep-quench regime such that their flow is first affected by  $P$  and then it reaches the fixed point  $Q$ .

In order to have a complete picture of the flow in the  $(\rho, g, \omega_0)$ -space which encompasses both the deep-quench regime  $\omega_0 \gg 1$  and the stationary one with  $\omega_0 \simeq 1$  one would need to extend the flow equation for  $\omega_0$  reported in Eq. (5) beyond the case  $\omega_0 \gg 1$ . However, this is difficult because corrections to Eq. (5) would induce a change of the Gaussian scaling towards the shallow quench regime and therefore they would inevitably imply the discussion of the corresponding dimensional crossover (reducing the upper critical dimensionality  $d_c$  from 4 to 3), which is still an open issue, both for quantum systems at finite temperature [61, 62] and for classical statistical systems in confined geometries [67].

## Appendix B: Equilibrium RG flow at finite temperature

The RG Eqs. (4) after a quench can be cast (with  $d_c = 4$ ) in the form [74]

$$\frac{dr}{d\ell} = 2r + uF(r) + \mathcal{O}(u^2), \quad (\text{B1a})$$

$$\frac{du}{d\ell} = \epsilon u + 3u^2 F'(0) + \mathcal{O}(u^3), \quad (\text{B1b})$$

where  $F(r) = F_Q(r) \equiv (a_d \Lambda^d/4) K_+(k)/\omega_k|_{k=\Lambda}$  depends on the factor  $K_+(k)/\omega_k$  which multiplies  $\cos(\omega_k t_-)$  in  $iC$  (see Eq. (3)). As we mentioned in the main text, this stationary contribution to  $iC$  turns into the correlation function of the system in equilibrium at temperature  $T = \beta^{-1}$  by replacing  $K_+$  in Eq. (3) with  $\coth(\beta\omega_k/2)$  [57]. Remarkably, it turns out that the RG equations for this latter case are simply given by Eqs. (B1) with  $F = F_{\text{eq}}(r) \equiv (a_d \Lambda^d/4) \coth(\beta\omega_k/2)/\omega_k|_{k=\Lambda}$ . A direct inspection of Eqs. (B1) shows that their fixed point is given by  $(r^*, u^*) = (\epsilon F(0)/[6F'(0)], -\epsilon/[3F'(0)]) + \mathcal{O}(\epsilon^2)$  (where we assume that no other parameter beyond  $r$  flows in  $F$ ), which render  $Q(\Omega_0) = (r_{\text{dy}}^*(\Omega_0), u_{\text{dy}}^*(\Omega_0))$  and  $Q_{\text{eq}}(T) = (r_{\text{eq}}^*(T), u_{\text{eq}}^*(T))$ , for  $F = F_Q(r)$  and  $F = F_{\text{eq}}(r)$ , respectively, discussed in the main text. A linearization of Eqs. (B1) shows that the eigenvalues of the stable ( $\mathbf{s}$ ) and unstable ( $\mathbf{u} = (1, 0) + \mathcal{O}(\epsilon)$ ) directions are given by  $-\epsilon$  and  $1/\nu_{\text{eq}}$ , independently of the form of  $F$ , which actually affects only  $\mathbf{s} \propto (-F(0), 2) + \mathcal{O}(\epsilon)$  via  $F(0)$ . Accordingly, at least up to this order in perturbation theory, the exponent  $\nu$  of the transition occurring either after the quench for fixed  $\Omega_0$  or in equilibrium at temperature  $T$  are the same, independently of  $\Omega_0$ ,  $T$ , and of the fact that the corresponding values of  $u^*$  differ generically. However, it is actually possible to define an effective temperature  $T = T_{\text{eff}}(\Omega_0)$  such that the systems which are critical after the quench (with  $\Omega_0$  constant) are critical also in equilibrium at temperature  $T_{\text{eff}}(\Omega)$ . In order for this to occur, it is necessary that the stable manifolds in the  $(\rho, g)$ -plane of the RG Eqs. (B1) with

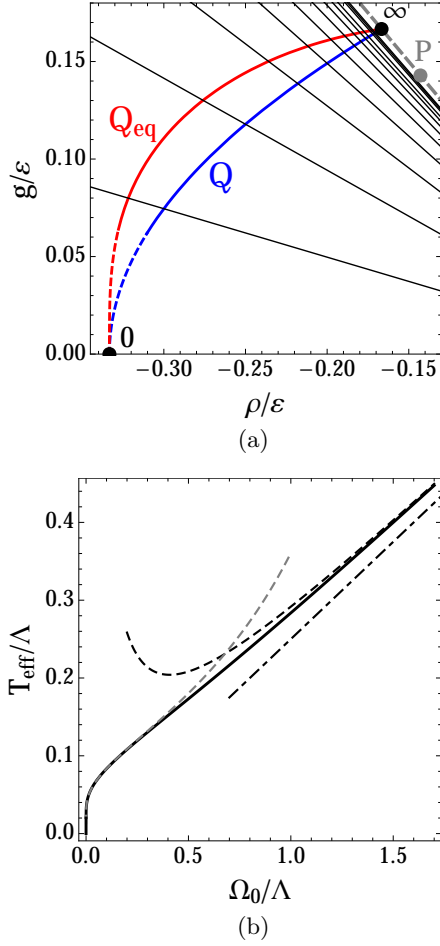


FIG. 4. (Color online) Comparison between the RG equations after a quench (with constant  $\Omega_0$ ) and those in equilibrium at temperature  $T$ . As explained in the main text, one can define an effective temperature  $T_{eff}(\Omega_0)$  for the system after the quench such that the corresponding fixed point  $Q(\Omega_0)$  has the same stable manifold as the equilibrium fixed point  $Q_{eq}(T_{eff}(\Omega_0))$ . Panel (a) shows  $Q(\Omega_0)$  and  $Q_{eq}(T_{eff}(\Omega_0))$  in the  $(\rho, g)$ -plane plotted parametrically by increasing  $\Omega_0/\Lambda$  from 0 to  $\infty$ , as indicated by the corresponding endpoints of the curves. For a given  $\Omega_0$ , the straight lines represent the common stable manifold of these two fixed points, with  $\Omega_0$  varying from 0.5 (lower line) to 6.5 (upper line) in steps of 0.5. For comparison, we report also the location of the deep-quench fixed point  $P$  (gray dot) and the corresponding stable manifold (gray dashed line). Panel (b) shows as a solid line the effective temperature  $T_{eff}$  as a function of  $\Omega_0$ , together with its asymptotic expressions for  $\Omega_0 \ll \Lambda$  (grey dashed curve) and  $\Omega_0 \gg \Lambda$  at the leading order (black dash-dotted line) and including the first correction (black dashed curve). See the main text for additional details.

$F = F_{eq}$  and  $F = F_Q$  are the same. After a linearization of Eqs. (B1) with fixed  $\Omega_0$  or  $T$ , these manifolds are straight lines, characterized by the direction  $\mathbf{s}$  and joining the corresponding fixed points with the Gaussian one  $G \equiv (0, 0)$ . Accordingly, up to  $\mathcal{O}(\epsilon)$  in perturbation theory, they coincide if  $\mathbf{s}|_{F=F_{eq}} = \mathbf{s}|_{F=F_Q}$ , i.e., if the condition  $F_Q(0) = F_{eq}(0)$  is fulfilled; this implies that  $Q(\Omega_0) - Q_{eq}(T_{eff}(\Omega_0))$  is along  $\mathbf{s}$  with, generically,  $Q(\Omega_0) \neq Q_{eq}(T_{eff}(\Omega_0))$ . The condition  $F_Q(0) = F_{eq}(0)$  amounts to requiring that

$$T_{eff}(\Omega_0) = \frac{\Lambda}{2} \left[ \ln \frac{\sqrt{1 + (\Omega_0/\Lambda)^2} + 1}{\sqrt{1 + (\Omega_0/\Lambda)^2} - 1} \right]^{-1}, \quad (B2)$$

which renders  $T_{eff}(\Omega_0 \gg \Lambda) = \Omega_0/4 + \Lambda^2/(24\Omega_0) + \mathcal{O}(\Lambda^4/\Omega_0^3)$  and  $T_{eff}(\Omega_0 \ll \Lambda) = \Lambda/[4 \ln(2\Lambda/\Omega_0)]$  as limiting cases. For a deep quench, this  $T_{eff}$  coincides with the one we have previously identified in the main text by requiring that the stationary part of  $iC$  after the quench resembles the one in equilibrium at temperature  $T_{eff}$ .

Figure 4(a) shows the location of the fixed points  $Q(\Omega_0)$  (lower solid blue curve) and  $Q_{eq}(T_{eff}(\Omega_0))$  (upper solid red curve) in the  $(\rho, g)$ -plane upon varying  $\Omega_0$  from 0 to  $\infty$ , as indicated at the corresponding endpoints of the two curves. The straight lines correspond to the common stable manifold of  $Q(\Omega_0)$  and  $Q_{eq}(T_{eff}(\Omega_0))$  for  $\Omega_0/\Lambda$  varying from 0.5 (lower straight line) to 6.5 (upper straight line) with increments in steps of 0.5. As we mentioned above, although  $T_{eff}(\Omega_0)$  has been determined in such a way that, for a fixed  $\Omega_0$ ,  $Q(\Omega_0)$  and  $Q_{eq}(T_{eff}(\Omega_0))$  have the same stable manifold, these two fixed points clearly differ but tend to coincide for  $\Omega_0 \gg \Lambda$ . In the opposite case of a shallow quench  $\Omega_0 \ll \Lambda$  (alternatively,  $T_{eff} \ll \Lambda$ ), instead, a dimensional crossover occurs which changes  $d_c$  from 4 to 3 in Eqs. (4) and it spoils the results of the dimensional expansion in the figure, as indicated by the dashed. For completeness we report also the position of the fixed point  $P$  of the deep-quench regime (gray dot) and the corresponding stable manifold (gray dashed line). Although, generically  $Q(\Omega_0)$  differs also from  $P$ , up to this order in perturbation theory, they share the stable manifold for  $\Omega_0 \gg \Lambda$ .

Figure 4(b) shows the effective temperature  $T_{eff}$  (solid line) in Eq. (B2) as a function of  $\Omega_0/\Lambda$ , together with its asymptotic behavior for  $\Omega_0/\Lambda \ll 1$  (grey dashed line) and for  $\Omega_0/\Lambda \gg 1$  both at the leading order, i.e.,  $T_{eff} = \Omega_0/4$  (black dash-dotted line) and upon including the first correction (black dashed line), which are all discussed above, after Eq. (B2).

- [1] A. Polkovnikov, K. Sengupta, A. Silva, and M. Vengalattore, *Rev. Mod. Phys.* **83**, 863 (2011).
- [2] A. Lamacraft and J. Moore, in *Ultracold Bosonic and Fermionic Gases*, edited by A. Fetter, K. Levin, and

- D. Stamper-Kurn (Elsevier, Oxford, 2012) Chap. 7.
- [3] V. Yukalov, *Laser Phys. Lett.* **8**, 485 (2011).
- [4] I. Bloch, J. Dalibard, and W. Zwerger, *Rev. Mod. Phys.* **80**, 885 (2008).

- [5] M. Greiner, O. Mandel, T. Esslinger, T. W. Hänsch, and I. Bloch, *Nature* **415**, 39 (2002).
- [6] M. Greiner, O. Mandel, T. W. Hansch, and I. Bloch, *Nature* **419**, 51 (2002).
- [7] J. M. Deutsch, *Phys. Rev. A* **43**, 2046 (1991).
- [8] M. Srednicki, *Phys. Rev. E* **50**, 888 (1994).
- [9] M. Rigol, V. Dunjko, and M. Olshanii, *Nature* **452**, 854 (2008).
- [10] J. Berges, S. Borsányi, and C. Wetterich, *Phys. Rev. Lett.* **93**, 142002 (2004).
- [11] T. Kitagawa, A. Imambekov, J. Schmiedmayer, and E. Demler, *New J. Phys.* **13**, 073018 (2011).
- [12] M. Gring, M. Kuhnert, T. Langen, T. Kitagawa, B. Rauer, M. Schreitl, I. Mazets, D. A. Smith, E. Demler, and J. Schmiedmayer, *Science* **337**, 1318 (2012).
- [13] T. Langen, R. Geiger, M. Kuhnert, B. Rauer, and J. Schmiedmayer, *Nature Physics* **9**, 640 (2013).
- [14] M. Kollar, F. A. Wolf, and M. Eckstein, *Phys. Rev. B* **84**, 054304 (2011).
- [15] M. Moeckel and S. Kehrein, *Phys. Rev. Lett.* **100**, 175702 (2008).
- [16] M. Moeckel and S. Kehrein, *Ann. Phys.* **324**, 21462178 (2009).
- [17] M. Moeckel and S. Kehrein, *New J. Phys.* **12**, 055016 (2010).
- [18] J. Marino and A. Silva, *Phys. Rev. B* **86**, 060408 (2012).
- [19] A. Mitra, *Phys. Rev. B* **87**, 205109 (2013).
- [20] M. van den Worm, B. C. Sawyer, J. J. Bollinger, and M. Kastner, *New J. Phys.* **15**, 083007 (2013).
- [21] M. Marcuzzi, J. Marino, A. Gambassi, and A. Silva, *Phys. Rev. Lett.* **111**, 197203 (2013).
- [22] T. Kinoshita, T. Wenger, and D. S. Weiss, *Nature (London)* **440**, 900 (2006).
- [23] M. Rigol, V. Dunjko, V. Yurovsky, and M. Olshanii, *Phys. Rev. Lett.* **98**, 050405 (2007).
- [24] A. Iucci and M. A. Cazalilla, *Phys. Rev. A* **80**, 063619 (2009).
- [25] E. T. Jaynes, *Phys. Rev.* **106**, 620 (1957).
- [26] T. Barthel and U. Schollwöck, *Phys. Rev. Lett.* **100**, 100601 (2008).
- [27] G. Goldstein and N. Andrei, arXiv:1405.4224.
- [28] B. Pozsgay, M. Mestyán, M. A. Werner, M. Kormos, G. Zaránd, and G. Takács, arXiv:1405.2843.
- [29] M. Mierzejewski, P. Prelovsek, and T. Prosen, arXiv:1405.2557.
- [30] B. Wouters, M. Brockmann, J. D. Nardis, D. Fioretto, and J.-S. Caux, arXiv:1405.0172.
- [31] F. H. L. Essler, G. Mussardo, and M. Panfil, arXiv:1411.5352.
- [32] J. Berges, A. Rothkopf, and J. Schmidt, *Phys. Rev. Lett.* **101**, 041603 (2008).
- [33] B. Nowak, D. Sexty, and T. Gasenzer, *Phys. Rev. B* **84**, 020506 (2011).
- [34] B. Nowak, J. Schole, and T. Gasenzer, *New J. Phys.* **16** (2014).
- [35] M. Kolodrubetz, B. K. Clark, and D. A. Huse, *Phys. Rev. Lett.* **109**, 015701 (2012).
- [36] A. Gambassi and A. Silva, arXiv:1106.2671.
- [37] A. Gambassi and A. Silva, *Phys. Rev. Lett.* **109**, 250602 (2012).
- [38] S. Sotiriadis, A. Gambassi, and A. Silva, *Phys. Rev. E* **87**, 052129 (2013).
- [39] E. G. Dalla Torre, E. Demler, and A. Polkovnikov, *Phys. Rev. Lett.* **110**, 090404 (2013).
- [40] B. Sciolla and G. Biroli, *Phys. Rev. Lett.* **105**, 220401 (2010).
- [41] A. Gambassi and P. Calabrese, *EPL (Europhysics Letters)* **95**, 66007 (2011).
- [42] B. Sciolla and G. Biroli, *J. Stat. Mech.: Theor. Exp.* **2011**, P11003 (2011).
- [43] B. Sciolla and G. Biroli, *Phys. Rev. B* **88**, 201110(R) (2013).
- [44] A. Chandran, A. Nandori, S. S. Gubser, and S. L. Sondhi, *Phys. Rev. B* **88**, 024306 (2013).
- [45] P. Smacchia, M. Knap, E. Demler, and A. Silva, arXiv:1409.1883.
- [46] M. Eckstein, M. Kollar, and P. Werner, *Phys. Rev. Lett.* **103**, 056403 (2009).
- [47] M. Schiró and M. Fabrizio, *Phys. Rev. Lett.* **105**, 076401 (2010).
- [48] H. K. Janssen, B. Schaub, and B. Schmittmann, *Z. Phys. B* **73**, 539 (1989).
- [49] P. Calabrese and A. Gambassi, *J. Phys. A: Math. Gen.* **38**, R133 (2005).
- [50] J. Bonart, L. F. Cugliandolo, and A. Gambassi, *J. Stat. Mech.: Theor. Exp.* **2012**, P01014 (2012).
- [51] M. Marcuzzi, A. Gambassi, and M. Pleimling, *EPL (Europhysics Letters)* **100**, 46004 (2012).
- [52] P. Gagel, P. P. Orth, and J. Schmalian, arXiv:1406.6387.
- [53] M. Buchhold and S. Diehl, arXiv:1404.3740.
- [54] H. W. Diehl, in *Phase Transitions and Critical Phenomena*, Vol. 10, edited by C. Domb and J. L. Lebowitz (Academic Press, London, 1986).
- [55] H. W. Diehl, *Int. J. Mod. Phys. B* **11**, 3503 (1997).
- [56] M. Pleimling, *J. Phys. A: Math. Gen.* **37**, R79 (2004).
- [57] G. Mahan, *Many-Particle Physics*, Physics of Solids and Liquids (Springer, 2000).
- [58] A. Kamenev, *Field Theory of Non-Equilibrium Systems* (Cambridge University Press, 2011).
- [59] P. Calabrese and J. Cardy, *J. Stat. Mech.: Theor. Exp.* **2007**, P06008 (2007).
- [60] M. Marcuzzi and A. Gambassi, *Phys. Rev. B* **89**, 134307 (2014).
- [61] S. Sachdev, *Quantum Phase Transitions*, 2nd ed. (Cambridge University Press, 2011).
- [62] S. L. Sondhi, S. M. Girvin, J. P. Carini, and D. Shahar, *Rev. Mod. Phys.* **69**, 315 (1997).
- [63] D. S. Fisher and P. C. Hohenberg, *Phys. Rev. B* **37**, 4936 (1988).
- [64] K. Wilson and J. Kogut, *Physics Reports* **12**, 75 (1974).
- [65] M. E. Fisher, *Rev. Mod. Phys.* **70**, 653 (1998).
- [66] A. Mitra, *Phys. Rev. Lett.* **109**, 260601 (2012).
- [67] J. L. Cardy, ed., *Finite-Size Scaling*, Current Physics Sources and Comments, Vol. 2 (Elsevier, 1988).
- [68] L. Foini, L. F. Cugliandolo, and A. Gambassi, *Phys. Rev. B* **84**, 212404 (2011).
- [69] L. Foini, L. F. Cugliandolo, and A. Gambassi, *J. Stat. Mech.: Theor. Exp.* **2011**, P09011 (2011).
- [70] A. Mitra and T. Giamarchi, *Phys. Rev. Lett.* **107**, 150602 (2011).
- [71] A. Mitra and T. Giamarchi, *Phys. Rev. B* **85**, 075117 (2012).
- [72] M. Tavora and A. Mitra, *Phys. Rev. B* **88**, 115144 (2013).
- [73] J. Lux, J. Müller, A. Mitra, and A. Rosch, *Phys. Rev. A* **89**, 053608 (2014).
- [74] A. Chiocchetta, M. Tavora, A. Gambassi, and A. Mitra, in preparation (2014).
- [75] P. Calabrese and J. Cardy, *Phys. Rev. Lett.* **96**, 136801 (2006).



- (2006).
- [76] M. Karl, B. Nowak, and T. Gasenzer, *Phys. Rev. A* **88**, 063615 (2013).
  - [77] W. S. Bakr, J. I. Gillen, A. Peng, S. Folling, and M. Greiner, *Nature* **462**, 74 (2009).
  - [78] W. S. Bakr, A. Peng, M. E. Tai, R. Ma, J. Simon, J. I. Gillen, S. Flling, L. Pollet, and M. Greiner, *Science* **329**, 547 (2010).
  - [79] I. Carusotto and C. Ciuti, *Rev. Mod. Phys.* **85**, 299 (2013).
  - [80] A. V. Gorshkov, M. Hermele, V. Gurarie, C. Xu, P. S. Julianne, J. Ye, P. Zoller, E. Demler, M. D. Lukin, and A. M. Rey, *Nature Physics* **6**, 289 (2010).
  - [81] X. Zhang, M. Bishof, S. L. Bromley, C. V. Kraus, M. S. Safronova, P. Zoller, A. M. Rey, and J. Ye, *Science* **345**, 1467 (2014).